

*Short note***Search for magnetic rotation in ^{202}Pb and ^{203}Pb**
 A. Görgen^{1,a}, H. Hübel¹, D. Ward², S. Chmel¹, R.M. Clark², M. Cromaz², R.M. Diamond², P. Fallon²,
 K. Hauschild^{3,b}, G.J. Lane², I.Y. Lee², A.O. Macchiavelli², and K. Vetter²
¹ Institut für Strahlen- und Kernphysik, Universität Bonn, Nussallee 14-16, D-53115 Bonn, Germany² Lawrence Berkeley National Laboratory, Berkeley, CA 94720, USA³ Lawrence Livermore National Laboratory, Livermore, CA 94550, USA

Received: 24 July 2000 / Revised version: 8 September 2000

Communicated by D. Schwalm

Abstract. High-spin states in ^{202}Pb and ^{203}Pb have been investigated by in-beam γ -ray spectroscopy following the reaction $^{198}\text{Pt}(^9\text{Be},\text{xn})$. A search for magnetic rotational bands in these isotopes confirmed one of the two bands previously assigned to ^{202}Pb and revealed a new band in this isotope. No evidence for magnetic rotation has been found in ^{203}Pb .

PACS. 21.60.-n Nuclear-structure models and methods – 23.20.Lv Gamma transitions and level energies – 27.80.+w $190 \leq A \leq 219$

Regular bands of magnetic dipole transitions have been observed in the Pb isotopes between ^{191}Pb and ^{202}Pb [1, 2]. The energy spacings of the states in these bands follow a rotational-like pattern over a wide spin range despite their very small deformation. Lifetime measurements [3–5] show that the $M1$ transitions are strongly enhanced whereas the $E2$ transition probabilities are very small as expected for almost spherical nuclei. On the other hand, the dynamical moments of inertia are rather large, resulting in ratios $\mathcal{J}^{(2)}/B(E2)$ which are more than an order of magnitude larger than in deformed nuclei.

The $M1$ bands in the Pb isotopes are based on high-spin proton excitations across the $Z = 82$ shell gap coupled to neutron-hole excitations in the $\nu i_{13/2}$ shell. The interaction favors a perpendicular orientation of the orbitals [6], resulting in a total angular momentum vector which points between the directions of the proton and neutron spins. Connected with this special coupling is a large perpendicular component of the magnetic dipole moment with respect to the total angular momentum axis. The rotation of this magnetic moment generates the strong $M1$ transitions. Therefore, this phenomenon has been named *Magnetic Rotation* [7]. With increasing angular momentum the proton and neutron spins align step-by-step into the direction of the total spin. As a consequence, the transverse component of the magnetic moment and, therefore,

the $B(M1)$ values decrease with increasing rotational frequency [3–5].

Magnetic rotational bands have been successfully described within the framework of the *Tilted Axis Cranking* (TAC) model [8]. In this model a uniform rotation about any axis, not necessarily a principal axis, of a deformed nucleus is considered. The deformation of the mean field is calculated to be slightly oblate with $\beta_2 \approx -0.1$ for the very neutron deficient Pb isotopes and $\beta_2 \approx -0.05$ for the heavier ones [9], in agreement with the small $B(E2)$ values [3]. TAC calculations suggest that some deformation is necessary for the formation of regular magnetic rotational bands. In a feedback mechanism the deformed field stabilizes the orientation of the proton and neutron high-spin orbitals, while, on the other hand, the spatial density distributions of these orbitals induce the deformation [10]. In an alternative approach, magnetic rotation has been described in terms of an effective interaction between the proton and neutron spins [11]. In this approach no deformation is needed to explain many features of the bands. Therefore, it is important to study the properties of magnetic rotational bands over a wide range of Pb isotopes with different deformations.

We have performed a search for magnetic rotational bands in ^{202}Pb and ^{203}Pb , which are the heaviest Pb isotopes accessible to heavy-ion-induced fusion reactions. High-spin states in both isotopes were populated by the reaction $^{198}\text{Pt}(^9\text{Be},\text{xn})^{202,203}\text{Pb}$ at a beam energy of 60 MeV. The beam was provided by the 88-Inch Cyclotron of the Lawrence Berkeley National Laboratory. Gamma-

^a e-mail: goergen@iskp.uni-bonn.de^b Present address: DAPNIA/SPhN, CEA Saclay, F-91191 Gif-sur-Yvette Cedex, France

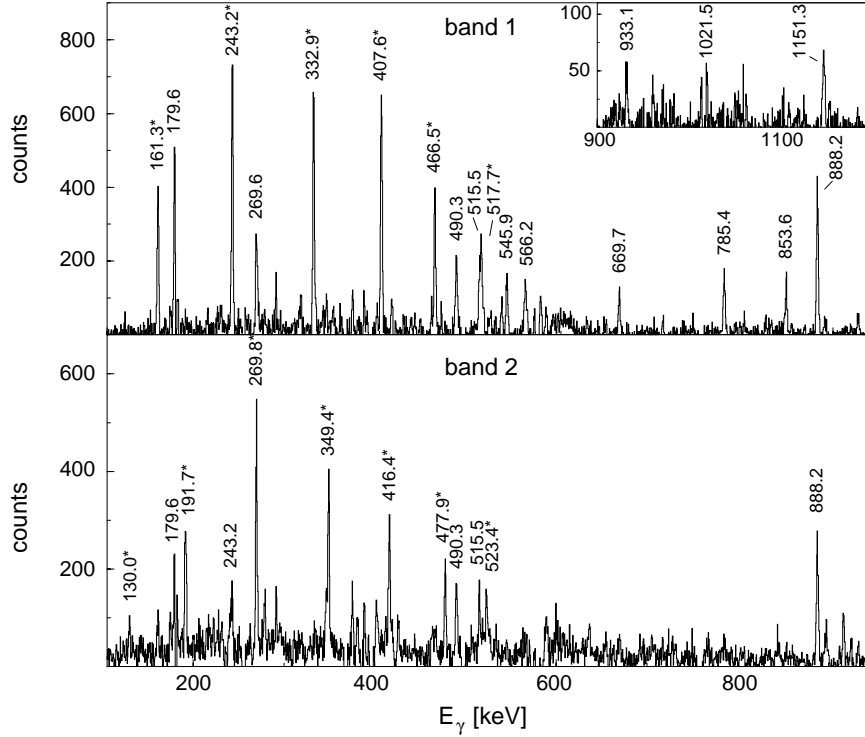


Fig. 1. Gamma-ray coincidence spectra showing band 1 and band 2 in ^{202}Pb . Both spectra are the sums of gates on the in-band transitions, which are marked by an asterisk.

rays were detected with the 8π spectrometer consisting of 20 Ge detectors with Compton suppression and an inner shell of 71 BGO scintillation detectors. Details of the experimental procedure are described elsewhere [12].

An earlier search for magnetic rotational bands in ^{202}Pb using the reaction $^{192}\text{Os}(^{14}\text{C},4n)$ revealed two bands [13]. However, the second band was only assigned tentatively to ^{202}Pb because the coincidence relations were not clear. Both bands were too weak for the determination

of DCO ratios and, therefore, no evidence for the dipole character of the transitions could be given.

Our data confirm the first band, and a new band, labeled band 2, was found. The second band reported in ref. [13] could not be confirmed. Gating on the suggested transitions revealed only lines belonging to ^{200}Hg , populated in the incomplete fusion channel [12], but no other in-band transitions. Either this band belongs to another nucleus not populated in the ^9Be reaction or it is simply not visible because the gates are contaminated by ^{200}Hg , which was not populated in the reaction used in ref. [13]. Spectra of bands 1 and 2 are shown in fig. 1. Energies, γ -ray intensities, total intensities corrected for internal conversion and DCO ratios for the two bands are summarized in table 1. DCO ratios were obtained using two different angular combinations as described in ref. [12] and are labeled R_{DCO}^A and R_{DCO}^B , respectively. The ratios R_{DCO}^A are normalized to the 888.2 and 840.7 keV transitions which are both of stretched $E2$ character, so that one expects $R_{\text{DCO}}^A = 1.0$ for stretched $E2$ and 0.66 for pure stretched dipole transitions. The ratios R_{DCO}^B of the in-band transitions were obtained by setting gates on other band members without normalization. These ratios are very sensitive to admixtures of higher multipoles and one expects $R_{\text{DCO}}^B = 0.69$ for a cascade of pure $M1$ transitions and 0.47 for a cascade with a constant $E2/M1$ mixing parameter $\delta = -0.1$. The DCO ratios given in table 1 show clearly the dipole character of the in-band transitions and the relatively small values of R_{DCO}^B indicate a small $E2$ admixture with negative sign, which means that the deformation is oblate [14], as expected.

Table 1. Energies, intensities and DCO ratios of the magnetic rotational bands in ^{202}Pb .

E_γ (keV)	I_γ	I_{tot}	R_{DCO}^A	R_{DCO}^B
<u>band 1</u>				
161.3	3.8(0.3)	13.5(1.1)	0.53(6)	0.41(7)
243.2	7.8(0.6)	14.1(1.1)	0.56(6)	0.38(6)
332.9	8.2(0.6)	11.0(0.8)	0.57(8)	0.32(5)
407.6	6.1(0.5)	7.3(0.6)	0.62(9)	0.34(5)
466.5	4.6(0.4)	5.2(0.4)	0.51(9)	0.34(8)
517.7	3.4(0.3)	3.8(0.3)	0.45(8)	–
<u>band 2</u>				
130.0	1.0(0.2)	5.7(1.1)	0.62(11)	–
191.7	2.2(0.2)	5.6(0.5)	0.62(7)	0.36(10)
269.8	3.5(0.3)	5.6(0.5)	0.58(6)	0.49(10)
349.4	3.0(0.3)	3.9(0.4)	0.61(7)	0.45(6)
416.4	2.7(0.2)	3.2(0.3)	0.57(8)	0.40(10)
477.9	1.8(0.2)	2.0(0.2)	0.46(8)	0.41(11)
523.4	1.6(0.2)	1.8(0.2)	0.49(10)	–

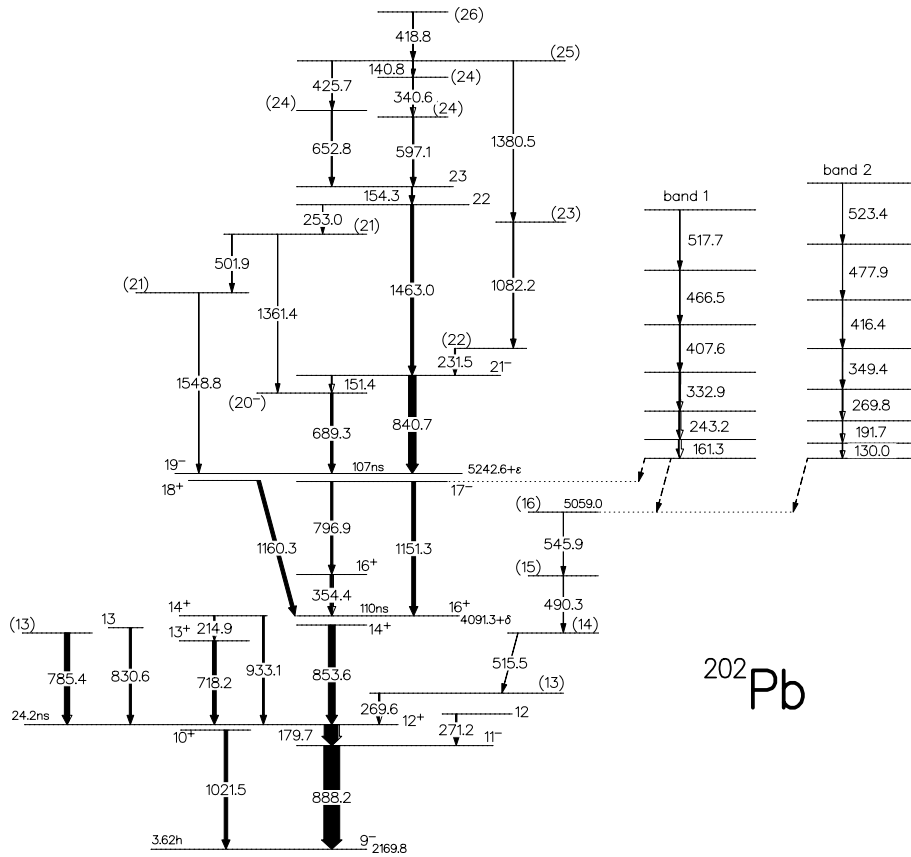


Fig. 2. Partial level scheme of ^{202}Pb . Most of the transitions and spin assignments below the isomeric state at 5.243+ ϵ MeV were adopted from previous work [15].

The level scheme of ^{202}Pb is shown in fig. 2. Most of the transitions and spin assignments below spin 19 were adopted from previous work [15], including the unobserved low-energy transitions below the isomeric states at 4.091+ δ MeV and 5.243+ ϵ MeV, respectively. Many new transitions have been found at high spins. The transition energies, intensities, DCO ratios, excitation energies and spin assignments of all transitions not belonging to one of the bands are listed in table 2. In most cases the ordering of the high-spin transitions is clear due to the observation of parallel decay paths. In all other cases the transitions were ordered according to their intensities. The DCO ratios of the transitions in the high-spin part do not allow an unambiguous spin assignment. In these cases the most likely spin values are given in parentheses.

It was not possible to link the bands to lower-lying states because the bands are weak and their decay is probably fragmented. Some intensity of the bands might be trapped in one of the many isomeric states. Therefore coincidences of delayed with prompt γ -rays were also analyzed, but without success. Both bands decay partly into the group of transitions with $E_\gamma = 545.9$, 490.3, 515.5 and 269.6 keV feeding the 12^+ isomeric state. Spin 16 is tentatively assigned to the highest-lying state in this group at 5.059 MeV. Band 1 is also in coincidence with the 1151.3 keV transition depopulating the 17^- state at 5.243+ δ MeV as can be seen in the inset of fig. 1. There-

fore, we assume that the band head of band 1 lies higher in excitation energy than 5.3 MeV and has a spin greater than 17. No other known transitions in ^{202}Pb were observed in coincidence with band 2, so that we can only give the excitation energy of the state at 5.059 MeV as a lower limit. Due to the lack of firm excitation energies and spin/parity assignments it is not possible to determine the nucleon configurations of the bands. In the lighter even-mass Pb isotopes the bands with the highest intensities have the AB11 and AE11 configurations [13, 16]. We may speculate that bands 1 and 2 in ^{202}Pb also have these configurations.

Only very few levels and transitions are known in ^{203}Pb from investigations using (α, xn) reactions [1]. In our experiment using a ^9Be beam we have populated states with higher spins compared to previous work and have observed several new transitions belonging to ^{203}Pb . However, the 4n channel leading to ^{203}Pb was only populated with 17% of the intensity of the 5n channel. Furthermore, many long-lived isomers make the analysis of coincidence relations difficult, so that the placement of the new lines is not clear. The inner ball of BGO detectors was used as a multiplicity filter and calorimeter to enhance high-spin transitions in ^{203}Pb , but no band structures with the features typical for magnetic rotation have been found.

Table 2. Energies, intensities, DCO ratios, excitation energies and spin assignments of the observed transitions in ^{202}Pb .

E_γ (keV)	I_γ	R_{DCO}^A	E_i (keV)	$I_i^\pi \rightarrow I_f^\pi$
140.8	2.7(0.4)	0.61(10)	8779.1+ ϵ	(25) \rightarrow (24)
151.4	1.6(0.4)	0.54(9)	6083.3+ ϵ	21 $^- \rightarrow$ (20 $^-$)
154.3	6.2(0.7)	0.49(8)	7700.6+ ϵ	23 \rightarrow 22
179.7	87.8(6.5)	0.63(6)	3237.7	12 $^+ \rightarrow$ 11 $^-$
214.9	4.0(0.4)	0.55(7)	4170.8	14 $^+ \rightarrow$ 13 $^+$
231.5	6.9(0.7)	0.62(7)	6316.4+ ϵ	(22) \rightarrow 21 $^-$
253.0	1.3(0.3)	–	7546.3+ ϵ	22 \rightarrow (21)
269.6	5.3(0.6)	0.76(14)	3507.3	(13) \rightarrow 12 $^+$
271.2	8.6(0.7)	0.51(6)	3329.2	12 \rightarrow 11 $^-$
340.6	4.2(0.4)	0.92(13)	8638.3+ ϵ	(24) \rightarrow (24)
354.4	16.9(1.3)	0.98(8)	4445.7+ δ	16 $^+ \rightarrow$ 16 $^+$
418.8	4.4(0.5)	0.59(8)	9197.9+ ϵ	(26) \rightarrow (25)
425.7	2.4(0.3)	0.62(9)	8779.1+ ϵ	(25) \rightarrow (24)
490.3	2.4(0.3)	0.48(14)	4513.1	(15) \rightarrow (14)
501.9	2.7(0.4)	0.79(18)	7293.3+ ϵ	(21) \rightarrow (21)
515.5	2.4(0.3)	0.50(14)	4022.8	(14) \rightarrow (13)
545.9	1.6(0.2)	0.51(16)	5059.0	(16) \rightarrow (15)
597.1	8.2(0.6)	0.56(8)	8297.7+ ϵ	(24) \rightarrow 23
652.8	7.3(0.6)	0.48(8)	8353.4+ ϵ	(24) \rightarrow 23
689.3	15.0(1.3)	0.33(9)	5931.9+ ϵ	(20 $^-$) \rightarrow 19 $^-$
718.2	20.9(1.6)	0.29(5)	3955.9	13 $^+ \rightarrow$ 12 $^+$
785.4	23.6(1.7)	1.01(9)	4023.1	(12) \rightarrow 12 $^+$
796.9	14.1(1.0)	0.65(15)	5242.6+ δ	17 $^- \rightarrow$ 16 $^+$
830.6	10.9(0.7)	0.63(8)	4068.3	13 \rightarrow 12 $^+$
840.7	47.2(2.9)	1	6083.3+ ϵ	21 $^- \rightarrow$ 19 $^-$
853.6	42.9(2.6)	1.06(8)	4091.3	14 $^+ \rightarrow$ 12 $^+$
888.2	100	1	3058.0	11 $^- \rightarrow$ 9 $^-$
933.1	8.0(0.7)	1.03(10)	4170.8	14 $^+ \rightarrow$ 12 $^+$
1021.5	5.6(0.5)	0.71(7)	3191.3	10 $^+ \rightarrow$ 9 $^-$
1082.2	6.0(0.7)	0.66(8)	7398.6+ ϵ	(23) \rightarrow (22)
1151.3	24.4(1.4)	0.66(7)	5242.6+ δ	17 $^- \rightarrow$ 16 $^+$
1160.3	5.8(0.4)	1.08(9)	5251.6+ δ	18 $^+ \rightarrow$ 16 $^+$
1361.4	0.7(0.3)	–	7293.3+ ϵ	(21) \rightarrow (20 $^-$)
1380.5	3.1(0.4)	0.80(20)	8779.1+ ϵ	(25) \rightarrow (23)
1463.0	19.3(1.1)	0.62(6)	7546.3+ ϵ	22 \rightarrow 21 $^-$
1548.8	3.8(0.5)	0.84(12)	6791.4+ ϵ	(21) \rightarrow 19 $^-$

Hole excitations in the $\nu i_{13/2}$ subshell are essential for the occurrence of magnetic rotation. The Fermi surface lies above this shell in the Pb isotopes with $A > 200$ and it takes more energy to excite $i_{13/2}$ neutrons. Therefore, one

can expect the magnetic rotational bands in the heavy Pb isotopes to lie higher in excitation energy than the bands in the lighter ones. Unfortunately, none of the bands in ^{200}Pb is connected to the lower-lying states [17], so that it is difficult to extrapolate excitation energies to ^{202}Pb . In ^{201}Pb one band is connected to lower-lying states with an excitation energy of 6.146 MeV [13], which is 2.3 MeV above the yrast state of the same spin. One can expect the corresponding excitation to lie even at higher energy in ^{203}Pb . Thus, it is not surprising that we did not observe magnetic rotational bands in this nucleus considering the limited efficiency of the 8π spectrometer.

This work was supported by BMBF (Germany) under contract no. 06BN907 and the U.S. DoE under contracts DE-AC03-76SF00098 (LBNL) and W-7405-ENG-48 (LLNL). A.G. acknowledges support from DAAD. The authors would like to thank the staff of the 88-Inch Cyclotron of the LBNL for providing the beam and David Radford for the RADWARE analysis package.

References

1. R.B. Firestone, V.S. Shirley, C.M. Baglin, S.Y.F. Chu, and J. Zipkin, (Editors), *Table of Isotopes* (J. Wiley and Sons, 1996).
2. Amita, A.K. Jain, B. Singh, *Atom. Data Nucl. Data* **74**, 283 (2000).
3. R.M. Clark et al., *Phys. Rev. Lett.* **78**, 1868 (1997).
4. R.M. Clark et al., *Phys. Lett. B* **440**, 251 (1998).
5. R. Krücken et al., *Phys. Rev. C* **58**, R1876 (1998).
6. S. Chmel et al., *Phys. Rev. Lett.* **79**, 2002 (1997).
7. S. Frauendorf, *Z. Phys. A* **358**, 163 (1997).
8. S. Frauendorf, *Nucl. Phys. A* **557**, 259c (1993).
9. S. Chmel, S. Frauendorf, H. Hübel, to be published.
10. S. Frauendorf et al., *Nucl. Phys. A* **601**, 41 (1996).
11. A.O. Macchiavelli et al., *Phys. Lett. B* **450**, 1 (1999) and references therein.
12. A. Görgen et al., *Eur. Phys. J. A* **6**, 141 (1999).
13. G. Baldsiefen et al., *Nucl. Phys. A* **592**, 365 (1995).
14. K. Nakai, *Phys. Lett. B* **34**, 269 (1971).
15. B. Fant et al., *Nucl. Phys. A* **475**, 338 (1987).
16. A. Görgen et al., *Nucl. Phys. A*, in press.
17. G. Baldsiefen et al., *Nucl. Phys. A* **574**, 521 (1994).